Pain Physician 2020; 23: E673-E686 • ISSN 2150-1149

Experimental Animal Study

Early Over-Expressing of microRNA-145 Effectively Precludes the Development of Neuropathic Mechanical Hyperalgesia via Suppressing Nav1.8 in Diabetic Rats

Jie Yan, MD[1], Huiling Yu, BA[2], Jie Shen, MD[1], Cuicui Han, BA[1], Caijuan Li, MD[1], Xiaofeng Shen, BA[1], and Bingbing Li, PhD[2]

From: [1]Department of Anesthesiology, Women's Hospital of Nanjing Medical University, Nanjing Maternity and Child Health Care Hospital, Nanjing, China; [2]Department of Anesthesiology, the Nanjing Drum Tower Hospital affiliated Nanjing University Medical School, Nanjing, China

Address Correspondence: Bingbing Li, PhD Department of Anesthesiology, the Nanjing Drum Tower Hospital affiliated Nanjing University Medical School, Zhongshan Road 321, Nanjing210008, China E-mail: icecolor@163.com

Disclaimer: This study was supported by the National Natural Science Foundation of China (project numbers: 81400913 and 81470242), the Six Talent Summit Project of Jiangsu Province (project number: WSN-147), and the Medical Science and Technique Development Foundation of Nanjing Municipal Government (QRX17013).

Conflict of interest: Each author certifies that he or she, or a member of his or her immediate family, has no commercial association (i.e., consultancies, stock ownership, equity interest, patent/licensing arrangements, etc.) that might pose a conflict of interest in connection with the submitted manuscript.

Manuscript received: 01-03-2020
Revised manuscript received: 04-09-2020
Accepted for publication: 05-08-2020

Free full manuscript: www.painphysicianjournal.com

Background: Painful diabetic neuropathy (PDN) is a common complication secondary to diabetes mellitus. Nav1.8 is an isoform of voltage-gated sodium channels and its expression regulation is closely related with PDN. MicroRNA-145 (miR-145) is involved in the occurrence and development of neuropathic pain. TargetScan software has revealed that Nav1.8 (SCN10A) is the major target of miR-145. However, its function between miR-145 and Nav1.8 in PDN is unknown.

Objectives: We aim to explore the regulatory effect of miR-145 on the expression and function of Nav1.8, which plays a pivotal role in precluding the advancement of neuropathic mechanical hyperalgesia in diabetic pain.

Study Design: An experimental, animal study.

Setting: An animal research facility at Nanjing Maternal and Child Health Institute, China.

Methods: The paw mechanical withdrawal threshold (PMWT) of rats was assessed with the von Frey test. The adverse regulation of Nav1.8 by miR-145 was confirmed by a dual luciferase detection system in HEK293T cells. The mRNA level and expression of Nav1.8 in dorsal root ganglion (DRG) neurons were assessed with real-time polymerase chain reaction (real-time PCR), western blotting and immunofluorescence assays following intrathecal injection of agomiR-145 in vitro and in vivo. Whole-cell patch-clamping was applied to assess alterations in the tetrodotoxin-resistant (TTX-R) sodium current (Nav1.8) in DRGs.

Results: The PMWT was significantly decreased in rats following streptozotocin (STZ) injection on Day 7 and was maintained at a lower level on Day 28; this change was accompanied by changes in the expression of Nav1.8 in DRG neurons, which was increased 3 days after STZ injection and reached a maximal level on Day 14. The early knockdown of Nav1.8 with siRNA or agomiR-145 treatment on Day 8 effectively precluded the deterioration of pain behaviors in STZ-treated rats. The luciferase intensity was significantly decreased in HEK293T cells expressing wild-type SCN10A infected with miR-145 mimic. In addition, Nav1.8 overexpression was significantly repressed via overexpression of miR-145 in cultured DRG neurons, and neuronal hyperexcitability was concomitantly decreased. Furthermore, the intrathecal administration of agomiR-145 elicited a significant decrease in Nav1.8 expression in DRG neurons from STZ-treated rats on Day 14.

Limitations: The causes of PDN are likely to be multifactorial and inflammatory markers, such as IL-6, IL-2, and TNF-α, are elevated in hyperglycemia and might be the precipitating factors that contribute to miR-145 dysregulation. The curative effect of miR-145 upregulation in reversal of pain behaviors at the stage of well-established PDN wasn't investigated in this study.

Conclusion: Early infection with a lentiviral vector overexpressing miR-145 adversely regulated the expression and function of TTX-resistant Nav1.8 and abrogated the development of PDN. Therefore, miR-145 might be a potential therapeutic target for preventing PDN in the near future.

Key word: Dorsal root ganglion, microRNA-145, Nav1.8, painful diabetic neuropathy

Pain Physician 2020: 23:E673-E686

Painful diabetic neuropathy (PDN), one of the common complications of the advanced stage of diabetes mellitus, is characterized by spontaneous pain, hyperalgesia and/or allodynia, exerting a severely negative impact on patients' physical activity (1-4). The traditional therapeutic options focus on controlling glycemic levels and pain with pharmacotherapy, which is frequently associated with intolerable side effects with increasing doses or upon the coadministration of diverse agents. Opioids are mostly ineffective for treating neuropathic pain and their chronic use is problematic. Therefore, it is of paramount importance to explore the precise pathogenesis of neuropathic pain and seek more effective and safer therapeutic options for PDN.

Voltage-gated sodium channels (VGSCs) are important ion channels expressed in dorsal root ganglion (DRG) neurons, and they play a pivotal role in nociceptive signal transmission and neuronal hyperexcitability (5,6). The Tetrodotoxin (TTX)-resistant VGSC 1.8 (Nav1.8), in which the α subunit encoded by the SCN10A gene, is preferentially expressed in small nociceptive fibers. A large number of studies have revealed that changes in Nav1.8 expression are associated with the development of inflammatory and neuropathic pain (7,8). In addition, Nav1.8 has been found to be specifically involved in the development of early diabetic neuropathy, contributing to allodynia and hyperalgesia to noxious mechanical or thermal stimuli (9,10). Thus, to discover key molecules that interact with DRG nociceptors in diabetic animal models of PDN.

MicroRNAs (miRNAs) are a class of noncoding ribonucleic acid (RNA) molecules 18~25 nucleotides in length. miRNAs are known to participate in almost every biological process, including cell proliferation, apoptosis, differentiation, and organogenesis, through sequence-specific binding to the 3'-untranslated region of a target mRNA and ultimately causing translational repression or degradation (11). Previous studies have suggested that miRNAs are involved in the etiology of neuropathic pain in several clinical settings and various rodent models (12-15). The relationship between miR-146a, miR-128a and PDN susceptibility was first proposed based on a study of 154 type II diabetes patients by Ciccacci and colleagues (16). Using microarray analysis, Gong and his colleagues first uncovered the differences in miRNA expression profiles between mice with diabetic neuropathic pain and normal mice (17). Upregulated expression of miR-29b and miR-106a can relieve axonal swelling and improve sensory and motor nerve conduction, respectively, in PDN rats (18,19). In addition, the decreased expression of miR-145 is related to nerve injury and can be used as a potential biomarker of the development of pain (20,21). The underlying role of miR-145 in other forms of neuropathic pain, in addition to its decreased expression that is relevant to fibromyalgia and pain caused by peripheral nerve injury, has also been investigated (22-24).

Given that Nav1.8 expression in DRG neurons plays an important role in PDN and that miR-145 is a key factor associated with pain, how miR-145 contributes to PDN remains to be elucidated. We hypothesized that miR-145 may be involved in the pathogenesis of neuropathic pain via the downregulation of Nav1.8 expression in DRG neurons. To our knowledge, our study is the first to delineate the relationship between miR-145 and Nav1.8 transcription and translation using a rat model of PDN. The present results indicate that miR-145 adversely regulates the expression of Nav1.8 and exerts a protective effect on PDN in diabetic rats induced by streptozotocin (STZ).

Methods

Animal Preparation and Induction of Peripheral Neuropathic Pain

Animals

Eight-week-old male Sprague-Dawley (SD) rats from Cavens Lab Animal Co, Ltd. (Changzhou, China) were housed under standard conditions (22 to 24° with a 12 hour/12 hour, light/dark cycle and 40 to 60% relative humidity). Water and food were freely accessed. Each cage housed 5 rats to prevent any effects of social isolation. All animal experiments were approved by the Animal Experiments Ethical Committee of the Obstetrics and Gynecology Hospital Affiliated with Nanjing Medical University and performed strictly in compliance with the requirements of the guidelines of the International Association for the Study of Pain (25). For each independent experiment, a total of 48 SD rats were randomly divided into 4 groups with 12 rats in each group; 36 STZ-treated rats received a single intrathecal injection of lentiviral vector on Day 8 or were left untreated. The other 12 rats were injected intraperitoneally (i.p.) with vehicle instead of STZ as the control group. The rats received isoflurane anesthesia prior to the intrathecal injection or tissue collection.

- **Induction of diabetes (26):** Diabetes was induced by a single i.p. injection of STZ (60 mg/kg; Sigma,

St. Louis, MO, USA) dissolved in 0.1 mol/L citrate buffer (pH 4.5).

- **Mechanical stimulus threshold test (27):** A series of von Frey filaments (North Coast Medical, Morgan Hill, CA) were used to evaluate reactions to nonnoxious, light touch of the hindpaw. The mechanical pain threshold was measured one day before and up to 28 days after STZ injection. The rapid withdrawal of the hindpaw after stimulation was defined as a positive response, and the paw withdrawal threshold was recorded in grams. The 50% mechanical PMWT was calculated according to Chaplan's up-down method (28). The mechanical stimulations were repeated 5 times at 5-minute intervals for each hindpaw.
- **Intrathecal injections and drug administration (29):** A 25-µl syringe and a BD PrecisionGlide 30-gauge, 1/2-inch needle were placed into the L5/6 intervertebral space of the rats. AgomiR-145 (one type of specially labeled and chemically-modified double-stranded microRNA mimicking endogenous microRNA) or its corresponding negative control with scrambling oligonucleotide sequence (agomiR-NC) drug solution was injected via intrathecal injection at a volume of 10 µL (20 µM) per rat. In addition, 10 µL containing 25 µg siRNA-Nav1.8 or siRNA-NC was delivered by intrathecal injection. siRNA-NC (as negative control for siRNA-Nav1.8 substituted for the randomized sequence of oligonucleotides), siRNA-Nav1.8 lentiviral vectors were purchased from BioshBio Co., Ltd. (Shanghai, China). The following sequence is the oligonucleotide sequence of agomiR-145: CACCTTGTCCTCACGGTCCAGTTTTCCCAGGAATCCCTTGGATGCTAAGATGGGGATTCCTGGAAATACTGTTCTTGAGGTCATGGCT (miRBase, MI0000918). The following sequences are the oligonucleotide sequences for siRNA-Nav1.8 or NC respectively: Forward, 5'-GUCCGAGUGUCACAAUCAAUU-3'; Reverse, 5'UUGAUUGUGACACUCGGACUU-3'. siRNA-NC: Forward, 5'-UUCUCCGAACGUGUCACGUdtdt-3', Reverse, 5'-ACGUGACACGUUCGGAGAA dtdt-3' (GenBank Accession NO NM-017247).

Immunofluorescence

Rats were deeply anesthetized with 2% isoflurane delivered via a nose cone on the 14th day post-STZ injection. All rats were then transcardially perfused with phosphate buffer solution (PBS) followed by 4% paraformaldehyde in 0.1 M phosphate buffer (PB, pH 7.4) under deep anesthesia. After perfusion, the L3-L5 DRG neurons were removed and embedded in optimal cutting temperature (OCT) and sectioned at a thickness of 5 µm with a freezing microtome (Leica, Germany). The frozen sections were incubated for 10 minutes in 3% H_2O_2/PBS at room temperature. Five sections from each rat were chosen at random for immunofluorescence staining. After 3 washes with PBS for 5 minutes, the sections were incubated with an anti-Nav1.8 primary antibody (1:200, Alomone Labs, Ltd, Jerusalem, Israel) overnight at 4°C. After 3 additional washes with PBS, the sections were then incubated with a CY3-conjugated goat anti-rabbit (1:200, Chemicon, Temecula, CA, USA) secondary antibody for 30 minutes at 37°C. All immunofluorescence-stained sections were examined with a Leica fluorescence microscope, and quantitative analysis of the fluorescence intensity was performed with Image-Pro Plus 6.0 (Media Cybernetics, Rockville, MD, USA).

Western Blot Analysis

After behavioral testing on the 14th day after STZ injection, 4 rats from each group were anesthetized with 2% isoflurane. Total protein of the L3-L5 DRG tissues were quickly dissected for use in subsequent western blotting. Western blotting was performed as previously described (30). For detection of target protein, horseradish peroxidase-conjugated secondary antibodies (1:1000, Danvers, MA, USA) were used and membranes were detected using ECL technology (Dingguo Biotech, Beijing, China) and captured digitally and analyzed quantitatively using an Image-Pro Plus 6.0 (Media Cybernetics, Rockville, MD, USA). The relative protein expression of Nav1.8 was normalized to the value of β-actin.

RNA Isolation and Quantitative Real-Time PCR

On the 14th day after STZ injection, 4 rats from each group were sacrificed. According to the manufacturer's instructions, total RNA of L3-5 DRG neurons were extracted using the TRIzol Total RNA Extraction Kit (Invitrogen, Carlsbad, CA, USA) and reverse transcribed into cDNA using a Thermo Scientific RevertAid First Strand cDNA Synthesis Kit(Thermo #K1622). qPCR was performed using a SYBR Green PrimeScript RT-PCR Kit (Thermo F-415XL,USA). Human U6 was used as an internal microRNA control, and GAPDH was used as an internal mRNA control. The following primers were used: miR-145 forward, 5'-ACACTCCAGCTGGGGT-

CCAGTTTTCCCAGGA-3′ and reverse, 5′-CTCAACTG-GTGTCGTGGAGTCG-CAATTCAGTTGAGAGGGATTC-3′; Nav1.8 forward, 5′-TGTTGCCT-GGCTCTGCTCTT-3′ and reverse, 5′-CCTTTGCGTGGGCATTCCTC-3′; and U6 forward, 5′-GCGCGTCGTGAAGCGTTC-3′ and reverse, 5′-GTGCAGGGTCCGAAAT-3′.The Applied Biosystems 7500 RealTime PCR System (ThermoFisher scientific, Carlsbad, CA, USA) was used to perform real-time PCR. All samples were run in triplicate. The $2^{-\Delta\Delta Ct}$ method was used to calculate the relative expression level of miR-145. ΔΔCt is defined as the subtraction of ΔCt value between the target gene and endogenous control in the control sample from ΔCt between the target gene and endogenous control in the test sample. Finally, fold-differences in gene expression between distinct samples were calculated using the $2^{-\Delta\Delta Ct}$.

Dual Luciferase Reporter Assay

To determine the direct relationships between the 3′-untranslated regions (3′UTR) of Nav1.8 (SCN10A) gene sequence and miR-145, the dual luciferase assay (Promega, Madison, WI, USA) was performed according to the manufacturer's instructions. A segment of 3′UTR of SCN10A containing the miR-145 binding site (wild type) or oligonucleotides containing mutated nucleotides in the seed-match sequence for miR-145 (mutant type) was amplified. Wild type (Wt) or mutant type (Mt) of SCN10A sequence were generated and cloned into pMIR luciferase reporter. HEK293T cells (1×10^5) were seeded on 96-well plates for 24h cultivation and then co-transfected with 10 μg of either Wt or Mt SCN10A reporter vectors, together with 100 nM of miR-145 mimics (artificially synthesized double-stranded RNA molecules serving as endogenous microRNA-145) using Lipofectamine 2000 reagent (Invitrogen) in each well. Forty-eight hours later, Dual-Glo lucifectamine reagent was added to each well and firefly luminescence was measured. Then Dual-Glo Stop & Glo reagent was added to each well, and Renilla luminescence was measured. The ratio of firefly activity to Renilla activity was recognized as relative reporter activity, which was counted repeatedly three times as the results of experiment.

DRG Neuron Dissociation and Culture

DRGs from L4-L6 vertebral column of fetal rats at gestational age of 16 d were dissected bilaterally and immediately transferred onto ice-cold oxygenated Dulbecco's modified Eagle's medium (DMEM). The ganglia were removed mechanically with fine spring scissors from connective tissue and incubated in enzyme solutions containing 1.0mg/mL collagenase D, 0.5mg/mL trypsin and 0.1mg/mL DNase for 35 minutes at 37°C and 1.25 mg/mL soybean trypsin inhibitor was added to inactive the enzyme. After mechanical and chemical disruption, DRG neurons were subsequently seeded into 35-mm diameter culture dishes and placed on the stage of an inverted microscope for at least 30 minutes.

Infection

Cultured neurons were plated in 6-well plates at a density of 5×10^6 cells/cm^2 for 24 h. Lentiviral Packaging Mix (LV-MAXTM System Biosciences Palo Alto, CA, USA) containing overexpressing miR-145, Nav1.8, and scrambled control were synthesized by Biosh Joint Medical Laboratory Center, Shanghai, China. The sequence information of overexpressing miR-145, Nav1.8 was provided by BioshBio Co., Ltd. The nucleotide segment was synthesized for lentiviral based overexpressing miR-145 in accordance with the mature sequence of miR-145: TTTTCCCAGGAATCCCTTGGA. The total length sequence of OpenReadingFrame of SCN10A (GenBank: NC_005107) was cloned followed by the construction of lentiviral vector for overexpressing Nav1.8. According to the manufacturer's instructions, DRG neurons were infected with various lentiviral vectors using Lipofectamine 2000 (Invitrogen). DRGs were assigned to 4 groups: control group (infected with scrambled control), Nav1.8 group (lentiviral vector overexpressing Nav1.8), miR-145 group (lentiviral vector overexpressing miR-145) and coinfection group (cotransfected with overexpressing Nav1.8 and miR-145). After 48 hours of infection, the cells were harvested and the infection efficiency of the DRGs in each group was detected. Coinfection with green fluorescent protein was performed to enable the visualization of the infected cells under confocal microscope equipped with a live cell apparatus (Olympus Corporation, Tokyo, Japan). Cells that emitted green fluorescence were selected for patch-clamp recording 24-48 hours later.

Patch-Clamp Recording

Whole-cell, patch-clamp recording was performed with an EPC-10 amplifier (HEKA Electronics, Germany) at room temperature. One μM TTX (Sigma) was added to a bath solution containing the following: 120 mM NaCl, 1 mM CsCl, 0.1 mM $CaCl_2$, 1 mM $MgCl_2$, 10 mM HEPES and 10 mM glucose, pH 7.4 with NaOH. Recording pipettes with a resistance of 6-8 MΩ were pulled from borosilicate glass by a 2-step microelectrode

puller P97 (Sutter Instruments, Novato, CA, USA) and were filled with the following reagents: 130 mM CsCl, 3 mM Na_2ATP_3, 3 mM $MgCl_2$, and 20 mM HEPES titrated with CsOH to pH 7.2. Seals (> 1 MΩ) between the electrode and cells were established. After the whole-cell configuration was established, the cell membrane capacitance and series resistance were compensated electronically by 70-80% to minimize voltage errors. Leak currents were subtracted using the online P/4 protocol. The data were sampled at 20 kHz and low-pass filtered at 5 kHz. Experimental data were collected and analyzed with PatchMaster Software (HEKA Electronics, Germany).

DRG neurons were held at -60 mV, and Nav1.8 currents were evoked by depolarizing pulses to -35 mV. The activation and inactivation properties of Nav1.8 currents were studied using appropriate voltage protocols. The voltage-clamp protocol consisted of 50-ms depolarizing steps from -55 mV to +20 mV in 5-mV increments and was used to determine the activation of Nav1.8 channels. The Boltzmann function of the form $G_{Na}/G_{Namax} = 1/\{1+\exp[(V_{m1/2} - V)/k]\}$ was used to describe the voltage dependence of activation, and the half-activation potential was obtained. The steady-state inactivation of the Nav1.8 channel was determined at a series of membrane potentials from -60 mV to -15 mV, in 5-mV increments for 500 ms and a subsequent test potential of -35 mV. The steady-state inactivation curve was fitted by the Boltzmann function $I/I = 1/\{1+\exp[(V - V_{m1/2})/k]\}$, where I_{Namax} is the maximal peak current and V is the prepulse membrane potential.

Statistical Analysis

The data are expressed as the mean ± standard error of mean (SEM) and were analyzed using SPSS 21.0 statistical analysis software (SPSS, Inc., Chicago, USA). All data were first tested for normal distribution and homogeneity of variance. If the samples conformed to a normal distribution and the generality variance of each sample was equal, the differences between 2 groups were analyzed by Student's t-test, and comparisons among multiple groups were analyzed using one-way analysis of variance (ANOVA) with Tukey's post-hoc test. A *P*-value of < 0.05 was considered statistically significant.

Results

1. Establishment of neuropathic pain in diabetic rats induced by STZ treatment: The rats were subjected to a single i.p. injection of STZ (60 mg/kg) to induce hyperglycemia. As shown in Fig. 1, the glycemic level was increased in STZ-treated rats 3 days after the injection compared with control rats and maintained at a high level (above 20 mmol/L) thereafter during the 28-day observational period. Consistent with previous results, the rats that received STZ treatment developed significant weight loss from Day 14 to Day 28 ($P < 0.05$). Notably, the PMWT of both hindpaws significantly decreased in rats that received STZ compared with control rats on Days 7, 14, 21, and 28 ($P < 0.001$), which indicated the successful establishment of a model of PDN.
2. Causative role of Nav1.8 in neuropathic pain in STZ-induced diabetic rats: Nav1.8 is considered to be predominantly involved in the pathogenesis of chronic neuropathic or inflammatory pain. In the present study, the time-course of the expression of Nav1.8 in DRG neurons in rats that received STZ injection was initially examined. The expression of Nav1.8 was significantly increased in rats 3 days following STZ injection and reached the maximal level on Day 14 (Fig. 2A). Furthermore, to explore the causative role of Nav1.8 in the formation of PDN, the rats received a single intrathecal administration of lentiviral vector expressing siRNA-Nav1.8 (10 μL, 1×10^6 TU/mL) on the 8th day after STZ treatment. We subsequently examined Nav1.8 expression on Day 14 and pain behaviors in diabetic rats after intervention with siRNA-Nav1.8 or scrambled siRNA. The upregulation of Nav1.8 in DRG neurons in STZ-treated rats was significantly suppressed by the knockdown of Nav1.8, which is consistent with the decrease in immunofluorescence intensity in DRG neurons from the siRNA-Nav1.8 group shown in Figs. 2B, C, E and F. Compared with STZ treatment, treatment with Nav1.8 siRNA markedly prevented the decrease in the PMWT (shown in Fig. 2D) for 12 successive days beginning on Day 10 (11.58 ± 0.35 vs 8.56 ± 0.38 g on Day 10, $P < 0.001$; 9.25 ± 0.29 vs 5.40 ± 0.22 g on Day 21, $P < 0.001$).
3 The protective role of miR-145 in neuropathic pain in STZ-treated diabetic rats: Neuropathic injury induces a large-scale remodeling of nociceptive neurons driven by long-term changes in gene expression. Therefore, a series of in vivo studies was conducted to investigate whether mechanical allodynia induced by diabetic neuropathy is associated with the downregulation of miR-145. First, the mRNA level of miR-145 in DRG neurons was significantly decreased in rats 3 days following STZ

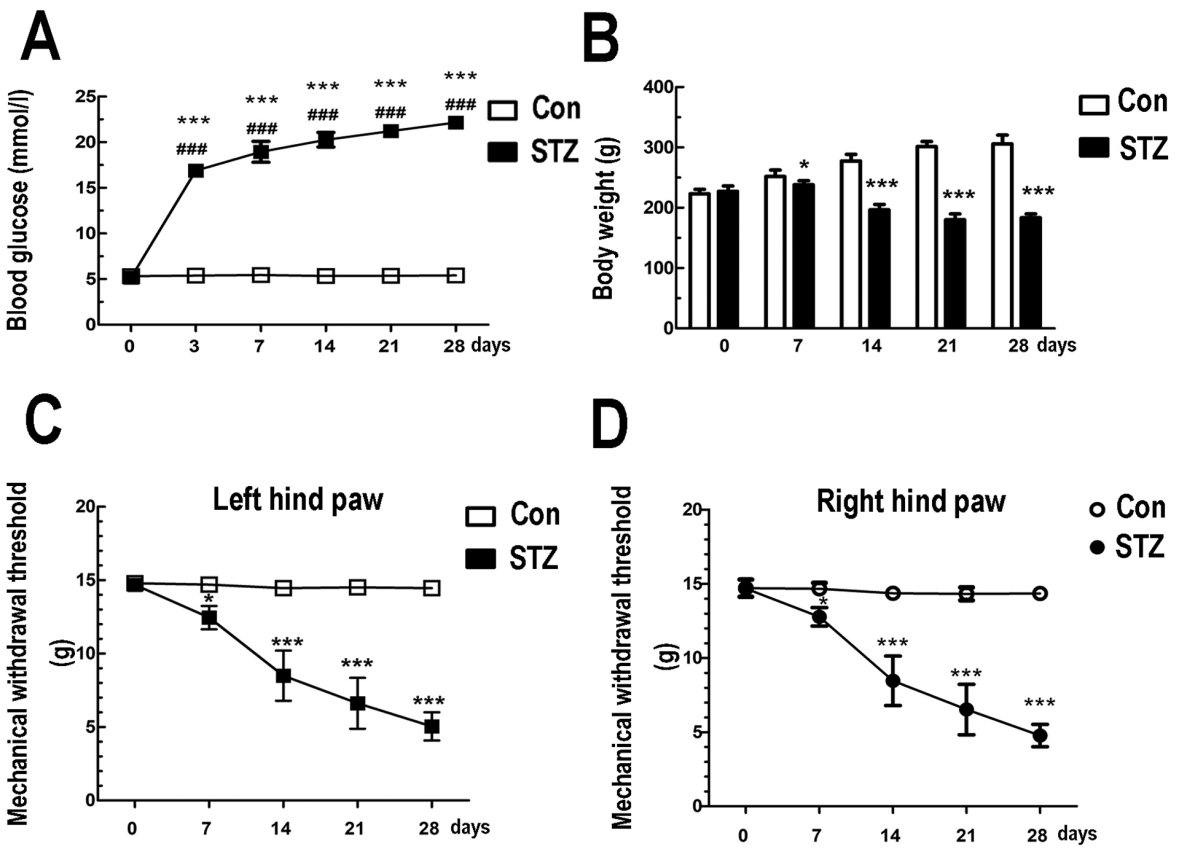

Fig. 1. *Establishment of a neuropathic pain model in diabetic rats induced by STZ treatment.*

A total of 24 Sprague-Dawley rats were randomly allocated to 2 groups with 12 rats per group. The rats in the STZ group were treated with a single intraperitoneal injection of STZ (60 mg/kg), whereas the rats in the control group received an equal volume of citrate buffer. The blood glucose level, body weight, and PMWT were measured on days 0, 7, 14, 21, and 28 after STZ treatment. The time-course of changes in blood glucose levels (A), body weight (B), and the PMWT of the left (C) and right hindpaw (D) were assessed. The data are expressed as the mean ± SEM (n = 12); $^{*}P < 0.05$, $^{**}P < 0.01$, $^{***}P < 0.001$ compared with control rats; $^{\#}P < 0.05$, $^{\#\#}P < 0.01$ compared with Day 0. STZ: streptozotocin; PMWT: paw mechanical withdrawal threshold.

injection (closed columns), reached the minimal level on Day 14, and was maintained at this level until Day 21. The open columns indicated the controlled rats who did not receive STZ insult and had no miR-145 downregulation in DRGs during the 21 day observational period (Fig. 3A). The STZ-treated rats were intrathecally injected with agomiR-145 (20 μM), scrambled agomiR-145, or a blank solution on Day 8. The miR-145 mRNA level in DRG neurons from diabetic rats treated with agomiR-145 was approximately 2.1-fold higher than that in DRG neurons from the STZ-treated group on Day 14 ($P < 0.01$ shown in Fig. 3B). Furthermore, the overexpression of miR-145, compared with STZ or scrambled siRNA treatment, markedly precluded the decrease in the PMWT on Day 21 (9.91 ± 0.41 vs 5.08 ± 0.46 g, $P < 0.001$; 9.91 ± 0.41 vs 5.13 ± 0.51 g, $P < 0.001$, respectively shown in Fig. 3C).

4. miR-145 directly targets SCN10A (Nav1.8) in rats: MicroRNAs inhibit the translation of specific genes by binding to the 3'UTR sequence of target messenger RNAs. To identify the miR-145 target gene relevant to pain, we used TargetScan (http://www.targetscan.org) to determine that the 3' UTR sequence of SCN10A---AGGAATC, can complementarily combine with the miR-145 5' seed region (Fig. 4A). A previous study (31) indicated that the Nav1.8 α-subunit is encoded by SCN10A. Therefore, a dual

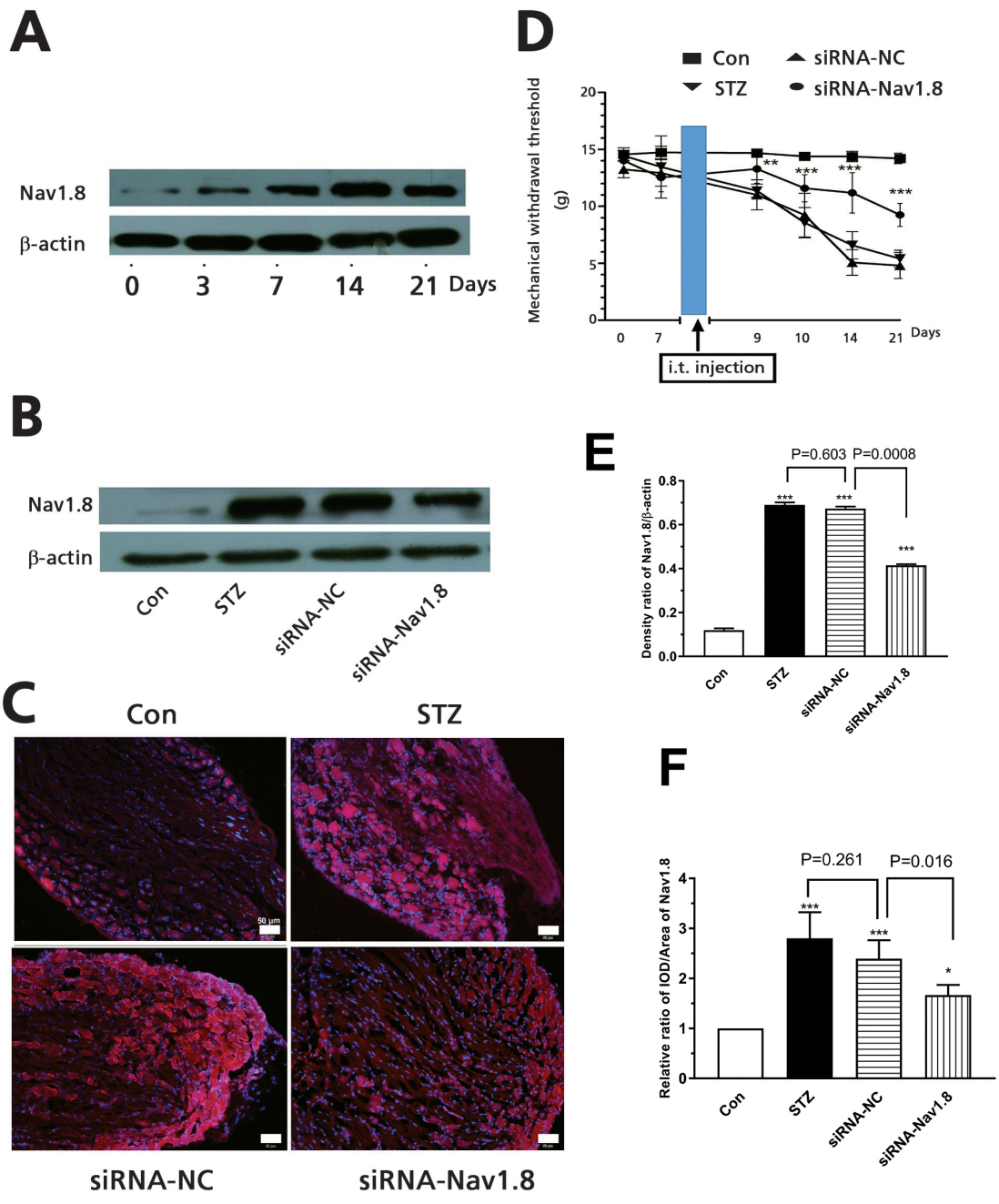

Fig. 2. *Causative role of Nav1.8 in neuropathic pain in STZ-induced diabetic rats.*

The expression profile of Nav1.8 over time was assessed by western blotting in rats that received STZ injection for 21 days. The representative change in Nav1.8 is shown in (A) based on identical results from 3 independent experiments. The rats received a single intrathecal injection of siRNA-Nav1.8, siRNA-NC, or vehicle on the 8th day after STZ treatment. The representative expression of Nav1.8 in DRG neurons on Day 14 after STZ treatment, as determined by western blotting (B) and immunofluorescence (C) (scale bar = 20 μm) is shown based on identical results from 3 separable experiments. The semi-quantitative analysis of Nav1.8 expression on Day 14 was shown in (E) and relative immunofluorescent intensity in (F) respectively. (D) The PMWT was assessed in rats subjected to intrathecal injection of siRNA-Nav1.8, siRNA-NC, or vehicle. The data are expressed as the mean ± SEM (n = 8). $^{*}P < 0.05$, $^{**}P < 0.01$, $^{***}P < 0.001$ compared with STZ-treated rats. Con: control; STZ: Streptozotocin; DRG: dorsal root ganglion neurons; i.t.: intrathecal; PMWT: paw mechanical withdrawal threshold; IOD, immunofluorescent optic density.

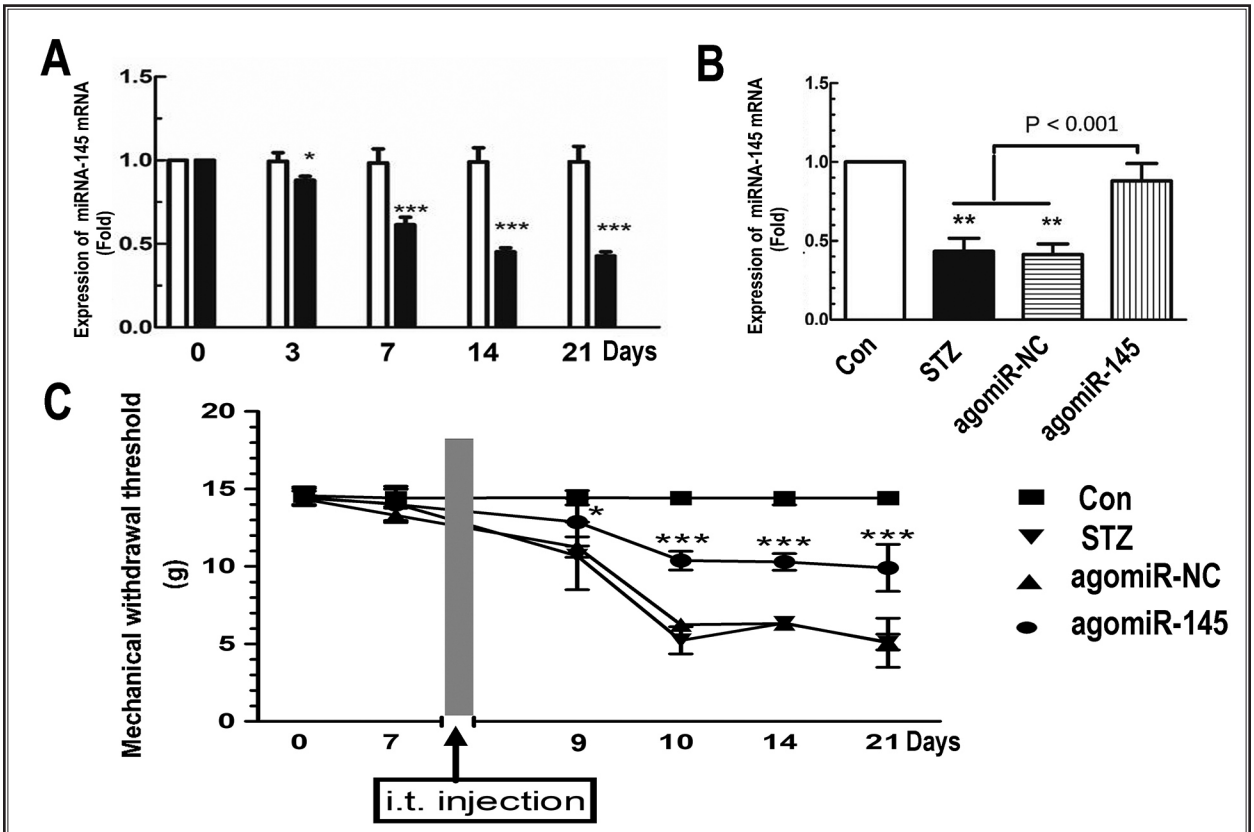

Fig. 3. *Protective role of miR-145 in neuropathic pain in STZ-treated diabetic rats.*

(A) Expression profile of miR-145 mRNA in rats treated with/without intraperitoneal STZ injection over time (n = 4). *$P < 0.05$, ***$P < 0.001$ vs. controlled rats. The rats received an intrathecal injection of agomiR-145, agomiR-NC, or vehicle on the 8th day after STZ treatment. The relative expression of miR-145 mRNA in DRG neurons from different groups on Day 14 is shown in (B) (n = 4). ** $P < 0.01$ vs controlled rats. (C) The PMWT was assessed in rats subjected to intrathecal injection of agomiR-145, agomiR-NC, or vehicle. The data are expressed as the mean ± SEM (n = 8). *$P < 0.05$, **$P < 0.01$, ***$P < 0.001$ compared with STZ-treated rats. STZ: streptozotocin; DRG: dorsal root ganglion neurons; PMWT: paw mechanical withdrawal threshold; i.t.: intrathecal.

luciferase reporter assay was used to confirm this interaction. HEK293T cells were cotransfected with Wt SCN10A (Nav1.8) together with miR-145 mimic or negative control miRNA. As expected, the luciferase intensity of cells bearing Wt SCN10A was attenuated by miR-145 treatment. In contrast, miR-145 did not affect the fluorescent intensity of the cells transfected by Mt SCN10A compared with the control ($P > 0.05$, Fig. 4B). These findings suggest that SCN10A is a target of miR-145.

5. Lentiviral infection with miR-145 elicits the down-regulation of Nav1.8 mRNA transcription and protein synthesis and its function in vitro and in vivo: To further validate the reciprocal relationship between miR-145 and Nav1.8, DRG neurons from normal embryonic rats were isolated and infected with a lentivirus expressing Nav1.8 with/without miR-145 for 48 hours. The Nav1.8 transcriptional level and subsequent protein expression were measured by real-time PCR and western blot assays, respectively. Infection with Nav1.8-expressing lentivirus resulted in 1.9-fold and 1.87-fold increases in the mRNA and protein levels, respectively, compared with that in control neurons. As shown in Fig. 5 A-C, the administration of miR-145 significantly decreased Nav1.8 mRNA levels as well as protein expression in neurons infected with the Nav1.8-expressing lentivirus ($P < 0.01$). To assess the functioning of the TTX-resistant sodium channel 1.8 subtype, whole-cell patch-clamp recording was performed. As shown in Fig. 5D, the

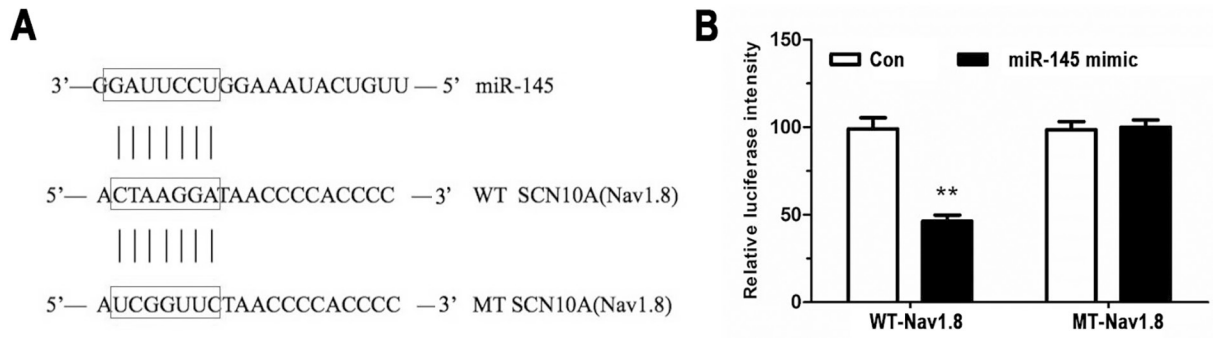

Fig. 4. *miR-145 directly targets SCN10A (Nav1.8) in rats.*

(A) Sequence alignment of miR-145 and rat SCN10A 3'UTR. The predicted alignment of the sequences of SCN10A 3'UTR and miR-145 are indicated by the red frame. (B) Luciferase activity of luciferase reporter genes bearing a wild-type or mutated-type Nav1.8 segment in HEK293T cells treated with or without miR-145 mimics. The data are expressed as the mean ± SEM (n = 3). *$P < 0.05$, **$P < 0.01$ compared with control cells.

mean peak current density in the DRG neurons overexpressing Nav1.8 was higher than in the Con group (–86.8 ± 0.9 vs 76.2 ± 1.2 pA/pF, $P < 0.05$, n =10), whereas, the lentivirus infection of miR-145 significantly decreased the peak current density of Nav1.8 in neurons treated with overexpressing Nav1.8 (-77.8 ± 0.6 vs -86.8 ± 0.9 pA/pF, $P < 0.05$, n = 10). The kinetics of activation were evaluated by curve fitting the rising phase of the conductance using a single exponential Boltzmann function (Fig. 5E). The midpoint of the voltage-dependence of activation was -10.0 ± 0.19 mV in neurons from normal rats and -10.4 ± 0.31 mV in neurons from rats treated with miR-145 overexpression alone. However, the values were significantly higher in the neurons exposed to Nav1.8 infection compared with control cells (-11.54 ± 0.36 vs -10.0 ± 0.19 mV; $P < 0.05$). Treatment with miR-145 elicited a depolarizing shift in the conductance-voltage curve to -10.6 mV in cells exposed to Nav1.8 ($P < 0.05$). As shown in Fig. 5F, the voltage dependence of steady-state inactivation was similarly calculated using the Boltzmann equation. The midpoints of steady-state inactivation were -40.53 ± 0.38 mV in control neurons and -39.67 ± 0.29 mV in neurons treated with miR-145 alone ($P > 0.05$). Additionally, the values were significantly higher in neurons exposed to Nav1.8 infection compared with control cells (-38.68 ± 0.27 vs -40.53 ± 0.38 mV; $P < 0.01$). Treatment with miR-145 overexpression elicited a negative shift in the steady-state inactivation TTX-R current to -39.24 ± 0.31 mV in cells exposed to Nav1.8 overexpression ($P < 0.05$).

Moreover, as shown in Fig. 6C and D, the expression of Nav1.8 protein in DRG neurons in diabetic rats on Day 14 was increased by approximately 4.5-fold compared with that in control rats and was significantly abrogated by agomiR-145 ($P < 0.01$). Consistent with the western blot results, our fluorescence experiment suggested that the expression of Nav1.8 in DRG neurons from diabetic rats was intensely upregulated compared with that in DRG neurons from control rats. In contrast to the rats treated with agomiR-NC, the immunofluorescence intensity of Nav1.8 was markedly suppressed by the intrathecal injection of agomiR-145 (Fig. 6A and B).

Discussion

Rodent models of diabetes induced by STZ have been widely applied for the study of the pathogenesis of neuropathic pain and for assessing the efficacies of new potential therapeutic drugs (32). Diabetic neuropathy commonly commences 7 days after STZ treatment, lasts as long as 56 days, and manifests as somatic sensory dysfunction, including thermal hyperalgesia and mechanical allodynia in rats (33). In the present study, the i.p. administration of STZ (60 mg/kg) resulted in a significant decline in the PMWT for both hindpaws during the period of 7~28 days after STZ treatment, which is characteristic of mechanical hyperalgesia in diabetic rats that develop PDN.

DRG neurons express multiple subtypes of voltage-gated sodium channels, predominantly Nav1.3, 1.7, 1.8, and 1.9. Nav1.8 channels are selectively expressed in small dorsal root nociceptor neurons and conduct the

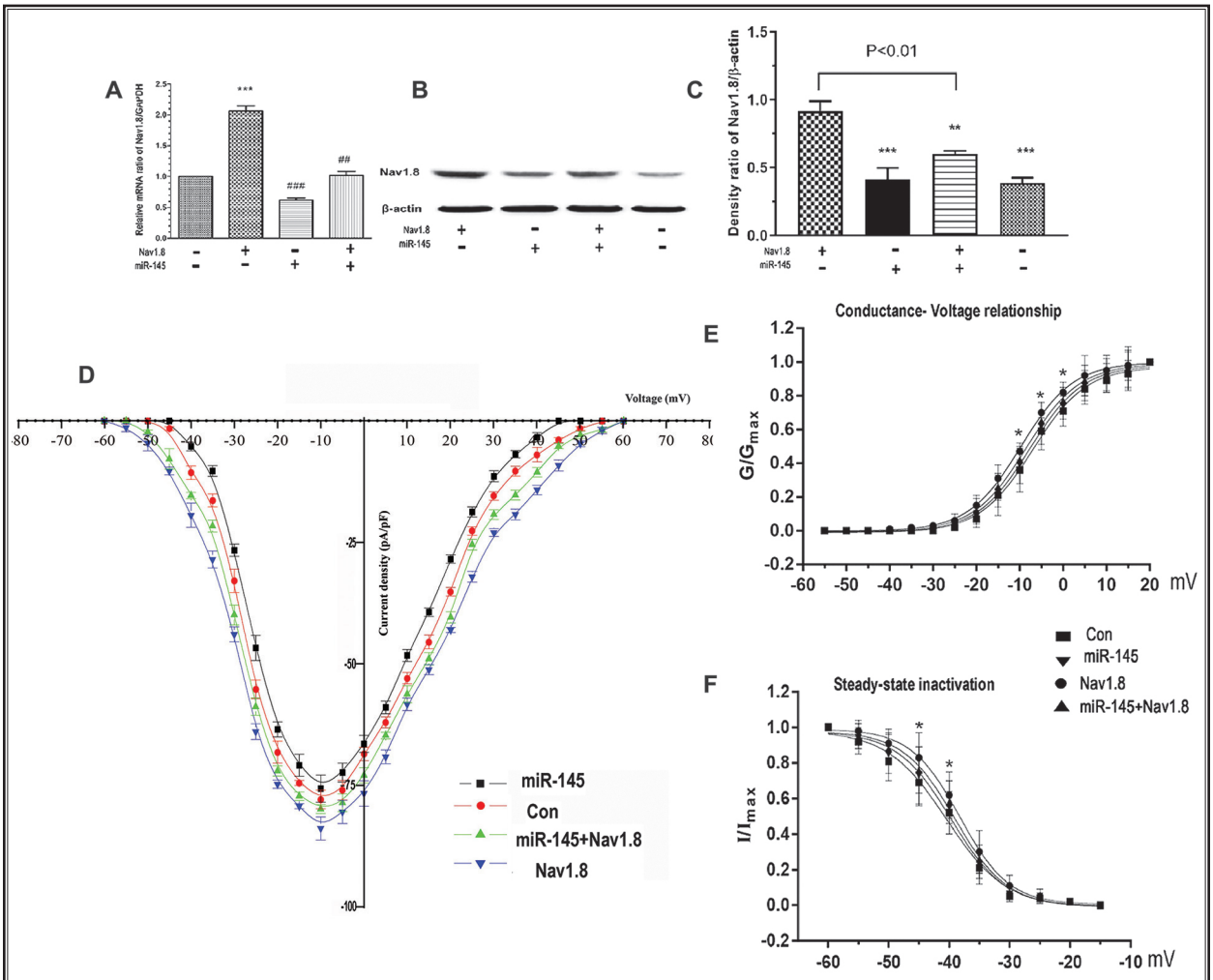

Fig. 5. *Effect of miR-145 on the expression of Nav1.8 and TTX-R sodium channel function in isolated DRG neurons.*

DRG neurons were infected with a lentiviral vector expressing Nav1.8 or miR-145 or exposed simultaneously to Nav1.8 and miR-145 for 48 h. The mRNA and total protein of DRG neurons were extracted. Real-time reverse transcription PCR was applied to determine the level of Nav1.8 mRNA (A), and western blotting was used to determine the expression of Nav1.8 (B). The semiquantitative analysis of Nav1.8 expression was shown in (C). The mean peak current density of Nav1.8 among 4 groups were plotted in (D). The normalized current-voltage curves of INa activation (E) and the steady state inactivation curve of TTX-R sodium channels (F) were plotted. The data are expressed as the mean ± SEM (n = 5). ***$P < 0.001$ vs controlled DRG neuron, #$P < 0.05$, ##$P < 0.01$, ###$P < 0.001$vs cell exposure to Nav1.8 overexpression. Con: control; TTX-R: Tetrodotoxin resistant; DRG: dorsal root ganglion.

majority of inward currents during an action potential (34). Although Nav1.8 channels play a crucial role in inflammatory pain states, their role in neuropathic pain is somewhat controversial. In the present study, we found that the protein level of Nav1.8 in DRG neurons was significantly increased in PDN rats throughout the 21-day observational period. Notably, the early knockdown of the expression of Nav1.8 via siRNA gene ablation precluded the excitatory firing of sensory nociceptors in rats treated with STZ, suggesting a causative role for Nav1.8 in the pathogenesis of PDN. A study by He and colleagues also indicated that the pharmacological ablation of Nav1.8 phosphorylation with rapamycin for 1 week has a beneficial effect in ameliorating PDN (35). In

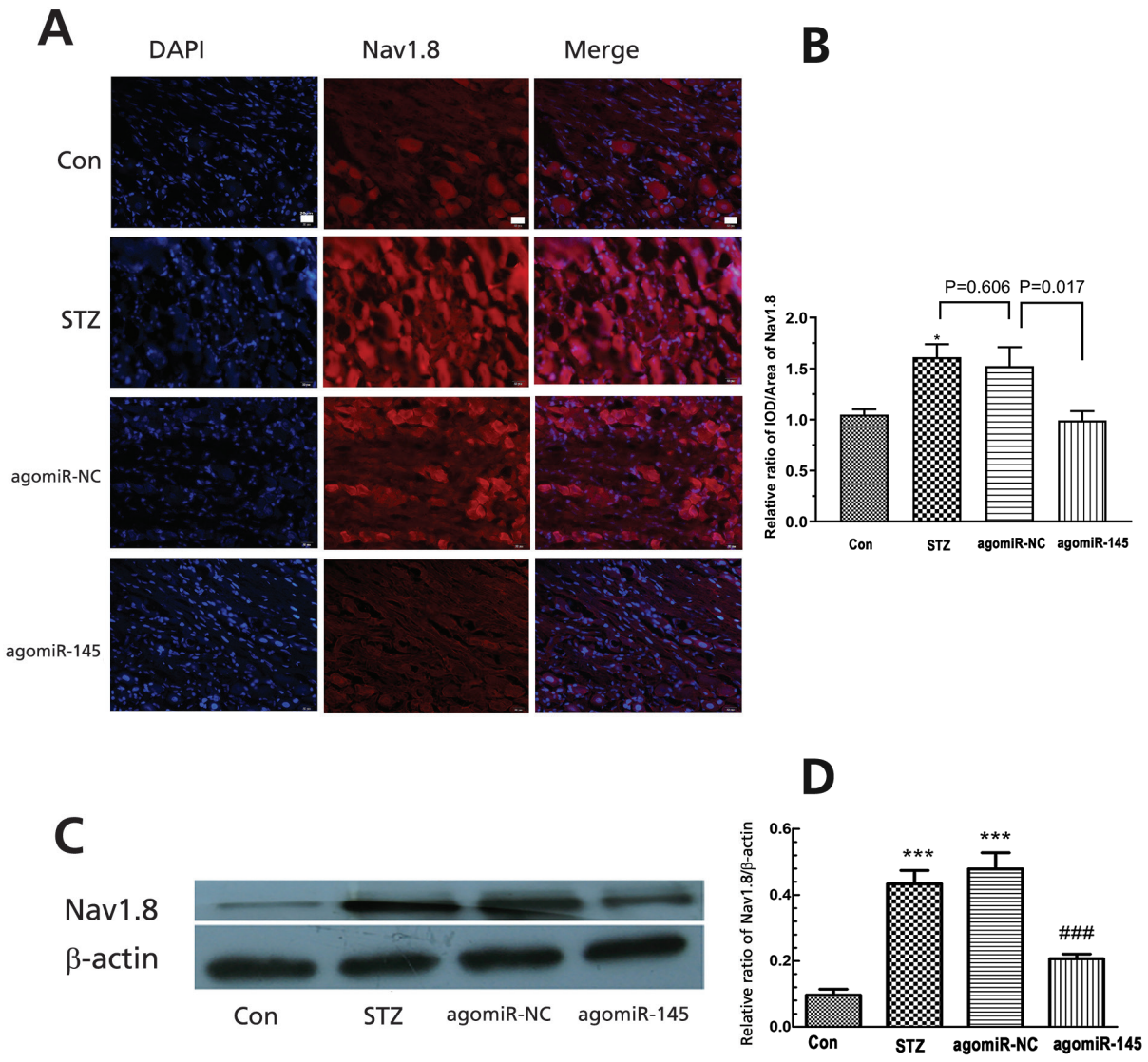

Fig. 6. *Effect of miR-145 on the alleviation of neuropathic pain in diabetic rats is associated with the downregulation of Nav1.8 expression in DRG neurons.*

The rats received an intrathecal injection of agomiR-145, agomiR-NC, or vehicle on the 8th day after STZ treatment. An immunofluorescence assay for Nav1.8 in DRG neurons from rats on the 14th day after STZ treatment is shown in (A) (scale bar = 20 μm) and semi-quantification of relative immunofluorescent intensity of Nav1.8 in (B). (C) The representative protein expression of Nav1.8 is shown based on identical result from 3 independent experiments. (D) Semiquantitative analysis of Nav1.8 expression in the different groups on Day 14. The data are expressed as the mean ± SEM (n = 3). $^{***}P < 0.001$ vs. control rats. $^{###}P < 0.001$ vs. STZ group. Con: control; STZ: Streptozotocin; DRG: dorsal root ganglion; IOD: immunofluorescent optic density.

He's study, the intervention was routinely commenced on the 21st day following STZ insult, when hyperalgesia or mechanic allodynia was found to be prominent in a majority of previous studies; thus, repeated doses were needed to overcome the relatively shorter duration of pain control. Unlike in the aforementioned studies, our intervention targeting upregulated Nav1.8 expression started as early as 8 days after STZ injection via a single intrathecal dose of siRNA-Nav1.8. The present results suggest that earlier intervention results in sustained

maintenance of normal pain behaviors in response to nonnoxious stimuli. Therefore, early recognition of diabetic patients susceptible to the development of PDN is of paramount importance because early therapeutic options offer sustained protection against the formation of PDN. Previous work has indicated that TTX-sensitive Nav1.7 sodium ions are responsible for almost half of the current in these DRG neurons, and an increase in the number of Nav1.7 channels allows for altered thresholds and spontaneous pain, which may be directly related to the occurrence and development of peripheral neuropathy. We cannot exclude the possibility that the abnormality of Nav1.8 channel expression and functioning might occur in advance of Nav1.7 upregulation in diabetic rats. Therefore, temporal heterogeneity in the expression of Nav1.7 and 1.8 in DRG neurons during the development of PDN needs further investigation.

Accumulating evidence has suggested that miRNAs are variably expressed in distinct rodent models of neuropathic pain disorders. Sakai et al (36) found that miR-7a is downregulated in injured DRG neurons in neuropathic pain, whereas miR-30b is suppressed in the DRG neurons of rats after chronic constriction injury (CCI) (37). Additionally, lower expression of miR-145 has been associated with pain in fibromyalgia and peripheral nerve injury. Our findings showed that the miR-145 expression level in DRG neurons was significantly decreased as early as 3 days after STZ treatment in rats. Early intervention with agomiR-145 significantly prevented the deterioration of hyperalgesia or allodynia in diabetic rats. In line with our results, pain-related behaviors are similarly relieved following the intrathecal injection of miR-145 in rats subjected to CCI (38). Many studies have confirmed that certain microRNAs are causally involved in the development of neuropathic pain through the regulation of voltage-gated sodium channel protein expression and neuronal excitability. A study by Chattopadhyzy indicated that reductions in Nav1.7 and 1.8 protein expression mediated by a virus-based vector expressing a microRNA targeting the α subunit of the Nav channel is related to a reduction in pain in diabetic rats (39). However, the mechanism by which miR-145 interacts with Nav1.8 in neuropathic pain has not been reported. Bioinformatics analysis using online software (TargetScan) demonstrated that Nav1.8 (SCN10A) mRNA is the target of miR-145. Our results strongly suggest that miR-145 adversely regulates the expression of Nav1.8 via binding to the 3'UTR region of Nav1.8. The evidence can be summarized as follows: 1) dual luciferase activity is inhibited after cotransfection with miR-145 and Wt Nav1.8 compared to the mutated Nav1.8 gene sequence in HEK293T cells; 2) the overexpression of miR-145 markedly reduces Nav1.8 mRNA transcription in DRG neurons treated with Nav1.8; 3) the protein expression levels of Nav1.8 in PDN rats are markedly decreased following intrathecal injection of agomiR-145; And 4) multitudes of evidence indicate Nav1.8 is associated with neuropathic pain signaling through its expression changes and altered electrophysiological properties. DRG neurons exposed to high glucose demonstrate a significant increase in the TTX-R Na^+ current. Nav1.8 activation produces an inward current during the depolarizing phase of the action potential via repetitive firing. The inhibition of TTX-resistant Nav1.8 channel activation or the acceleration of its steady-state current inactivation was achieved by lentiviral infection with miR-145 for 48 hours in the present study.

There are still several limitations we have to address in the present study: 1) the causes of PDN are likely to be multifactorial, and inflammatory markers, such as IL-6, IL-2, and TNF-α, are elevated in hyperglycemia and might be the precipitating factors that contribute to miR-145 dysregulation. The causative role of these cytokines or acute hyperglycemia contributing to pathologic exacerbation in peripheral nerve tissue in PDN mediated by magnified inflammation or oxidative stress needs to be elucidated; 2) in addition, 2 isoforms of VGSCs, NaV1.3 and NaV1.7 have been identified in both peripheral nociceptive neurons of DRGs and serve as an important participant involving in the formation of PDN. The relationship between these VGSCs in the pathogenesis of PDN, especially their roles in the distinct stage of this chronic pathologic process deserves further investigation; 3) lastly, the early intervention of downregulating Nav1.8 has the preventive effect in hyperglycemia induced mechanical hyperalgesia, however, its curative effect on hyperalgesia when PDN is completely established hasn't been delineated in this study.

Conclusion

The present study revealed that miR-145-mediated Nav1.8 downregulation may contribute to relieving pain in PDN. These findings indicate that early intervention in the miR-145-Nav1.8 axis in DRGs may be a potential strategy for the prevention and treatment of PDN.

Ethics approval

All animal experiments were approved by the Animal Experiments Ethical Committee of the Obstetrics and Gynecology Hospital Affiliated with Nanjing Medical University (file no. [2015]114).

Availability of data and materials

All data generated or analyzed during this study are included in the published article.

References

1. Dyck PJ, Albers JW, Andersen H, et al. Diabetic polyneuro-pathies: Update on research definition, diagnostic criteria and estimation of severity. *Diabetes Metab Res Rev* 2011; 27:620-628.
2. Swislocki A, Orth M, Bales M, et al. A randomized clinical trial of the effectiveness of photon stimulation on pain, sensation, and quality of life in patients with diabetic peripheral neuropathy. *J pain Sympt Manage* 2010; 39:88-99.
3. Finnerrup NB, Attal N, Haroutounian S, et al. Pharmacotherapy for neuropathic pain in adults: A systematic review and meta-analysis. *Lancet Neurol* 2015; 14:162-173.
4. Javed S, Petropoulos IN, Alam U, Malik RA. Treatment of painful diabetic neuropathy. *Therap Adv Chronic Dis* 2015; 6:15-28.
5. Rogers M, Tang L, Madge DJ, Stevens EB. The role of sodium channels in neuropathic pain. *Semin Cell Dev Biol* 2006; 17:571-581.
6. Emery EC, Luiz AP, Wood JN. Nav1.7 and other voltage-gated sodium channels as drug targets for pain relief. *Expert Opin Ther Targets* 2016; 20:975-983.
7. Lai J, Gold MS, Kim CS, et al. Inhibition of neuropathic pain by decreased expression of the tetrodotoxin sodium channel, Nav1.8. *Pain* 2002; 95:143-152.
8. Henry MA, Freking AR, Johnson LR, Levinson SR. Increased sodium channel immunofluo-rescence at myelinated and demyelinated sites following an inflammatory and partial axotomy lesion of the rat infraorbital nerve. *Pain* 2006; 124:222-233.
9. Leo S, D'Hooge R, Meert T. Exploring the role of nociceptor-specific sodium channels in pain transmission using Nav1.8 and Nav1.9 knockout mice. *Behav Brain Res* 2010; 208:149-157.
10. Kharatmal SB, Singh JN, Sharma SS. Voltage-Gated sodium channels as therapeutic targets for treatment of painful diabetic neuropathy. *Mini Rev Med Chem* 2015; 15:1134-1147.
11. Jones DZ, Schmidt ML, Suman S, et al. Micro-RNA-186-5p inhibition attenuates proliferation, anchorage independent growth and invasion in metastatic prostate cancer cells. *BMC Cancer* 2018; 18:421.
12. Lôpez-Gonzâlez MJ, Landry M, Favereaux A. MicroRNA and chronic pain: From mechanisms to therapeutic potential. *Pharmacol* 2017; 180:1-15.
13. Sakai A, Suzuki H. Emerging roles of microRNAs in chronic pain. *Neurochem Int* 2014; 77:58-67.
14. Sakai A, Suzuki H. microRNA and pain. *Adv Exp Med Biol* 2015; 888:17-39.
15. Ito N, Sakai A, Miyake N, et al. miR-15b mediates oxaliplatin-induced chronic neuropathic pain through BACE1 downregulation. *Br J Pharmacol* 2017; 174:386-395.
16. Ciccacci C, Morganti R, Di Fusco D, et al. Common polymorphrisms in miR146a, miR128a and miR27a genes contribute to neuropathy susceptibility in type 2 diabetes. *Acta Diabetol* 2014; 51:663-671.
17. Gong Q, Lu Z, Huang Q, et al. Altered microRNAs expression profiling in mice with diabetic neuropathic pain. *Biochem Biophys Res Commun* 2015; 456:615-620.
18. Zhang X, Gong X, Han SH, Zhang Y. MiR-29b protects dorsal root ganglia neurons from diabetic rat. *Cell Biochem Biophy* 2014; 70:1105-1111.
19. Wu Y, Xu D, Zhu X, Yang G, Ren M. miR-106a associated with diabetic peripheral neuropathy through the regulation of 12/15-LOX-mediated oxidative/nitrative stress. *Curr Neurovasc Res* 2017; 14:117-124.
20. Lu A, Huang Z, Zhang C, et al. Differential expression of microRNAs in dorsal root ganglia after sciatic nerve injury. *Neural Regen Res* 2014; 9:1031-1040.
21. Lecchi C, Dalla Costa E, Lebelt D, et al. Circulating miR-23b-3p, miR-145-5p and miR-200b-3p are potential biomarker to monitor acute pain associated with laminitis in horses. *Animal* 2018; 12:366-375.
22. Bjersing JL, Lundborg C, Bokarewa MI, Mannerkorpi K. Profile of cerebrospinal microRNAs in fibromyalgia. *PloS One* 2013; 8:e78762.
23. Zhang HY, Zheng SJ, Zhao JH, et al. MicroRNAs 144,145 and 214 are down-regulated in primary neurons responding to sciatic nerve transection. *Brain Res* 2011; 1383:62-70.
24. Norcini M, Sideris A, Martin Hernandez LA, Zhang J, Blanck TJ, Recio-Pinto E. An approach to identify microRNAs involved in neuropathic pain following a peripheral nerve injury. *Front Neurosci* 2014; 8:266.
25. Zimmermann M. Ethical guidelines for investigations of experimental pain in conscious animals. *Pain* 1983; 16:109-110.
26. Yao L, Wu YT, Tian GX, Xia CQ, Zhang F, Zhang W. Acrolein scavenger hydralazine prevents streptozotocin-induced painful diabetic neuropathy and spinal neuroinflammation in rats. *Anat Rec (Hoboken)* 2017; 300:1858-1864.
27. Dixon WJ. Efficient analysis of experimental observations. *Annu Rev Pharmacol Toxicol* 1980; 20:441-462.
28. Chaplan SR, Bach FW, Pogrel JW,

Chung JM, Yaksh TL. Quantitative assessment of tactile allodynia in the rat paw. *J Neurosci Methods* 1994; 53:55-63.

29. Hylden JL, Wilcox GL. Intrathecal morphine in mice: A new technique. *Eur J Pharmacol* 1980; 67:313-316.
30. Tanaka KI, Sekino S, Ikegami M, Ikeda H, Kamei J. Antihyperalgesic effects of ProTx-II, a Nav1.7 antagonist, and A803467, a Nav1.8 antagonist, in diabetic mice. *J Exp Pharmacol* 2015; 7:11-16.
31. Zhang L, Zhou F, Huang L, et al. Association of common and rare variants of SCN10A gene with sudden unexplained nocturnal death syndrome in Chinese Han population. *Int J Legal Med* 2017; 131:53-60.
32. Mert T, Oksuz H, Tugtag B, Kilinc M, Sahin E, Altun I. Anti-hypernociceptive and antioxidative effects of locally treated dobutamine in diabetic rats. *Pharmacol Rep* 2015; 67:1016-1023.
33. Sun W, Miao B, Wang XC, et al. Gastrodin inhibits allodynia and hyperalgesia in painful diabetic neuropathy rats by decreasing excitability of nociceptive primary sensory neurons. *PloS One* 2012; 7:e39647.
34. Xiao Y, Barbosa C, Pei Z, et al. Increased resurgent sodium currents in Nav1.8 contribute to nociceptive sensory neuron hyperexcitability associated with peripheral neuropathies. *J Neurosci* 2019; 39:1539-1550.
35. He WY, Zhang B, Xiong QM, et al. Intrathecal administration of rapamycin inhibits the phosphorylation of DRG Nav1.8 and attenuates STZ-induced painful diabetic neuropathy in rats. *Neurosci Lett* 2016; 619:21-28.
36. Sakai A, Saitow F, Miyake N, Miyake K, Shimada T, Suzuki H. miR-7a alleviates the maintenance of neuropathic pain through regulation of neuronal excitability. *Brain* 2013; 136:2738-2750.
37. Su S, Shao J, Zhao Q, et al. MiR-30b attenuates neuropathic pain by regulating voltage-gated sodium channel Nav1.3 in rats. *Front Mol Neurosci* 2017; 10:126.
38. Pang X, Tang Y, Zhang D. Role of miR-145 in chronic constriction injury. *Exp Ther Med* 2016; 12:4121-4127.
39. Chattopadhyay M, Zhou Z, Hao S, Mata M, Fink DJ. Reduction of voltage gated sodium channel protein in DRG by vector mediated miRNA reduces pain in rats with painful diabetic neuropathy. *Mol Pain* 2012; 8:17.